J Neurophysiol 94: 2713–2725, 2005.
First published June 29, 2005; 10.1152/jn.00024.2005.

Characteristic Membrane Potential Trajectories in Primate Sensorimotor Cortex Neurons Recorded In Vivo

Daofen Chen,[1,2] and Eberhard E. Fetz[2]

[1]*Systems and Cognitive Neuroscience, National Institute of Neurological Disorders and Stroke, Bethesda, Maryland; and* [2]*Department of Physiology and Biophysics, Washington National Primate Research Center, University of Washington School of Medicine, Seattle, Washington*

Submitted 10 January 2005; accepted in final form 26 June 2005

Chen, Daofen and Eberhard E. Fetz. Characteristic membrane potential trajectories in primate sensorimotor cortex neurons recorded in vivo. *J Neurophysiol* 94: 2713–2725, 2005. First published June 29, 2005; 10.1152/jn.00024.2005. We examined the membrane potentials and firing properties of motor cortical neurons recorded intracellularly in awake, behaving primates. Three classes of neuron were distinguished by *1*) the width of their spikes, *2*) the shape of the afterhyperpolarization (AHP), and *3*) the distribution of interspike intervals. Type I neurons had wide spikes, exhibited scoop-shaped AHPs, and fired irregularly. Type II neurons had narrower spikes, showed brief postspike afterdepolarizations before the AHP, and sometimes fired high-frequency doublets. Type III neurons had the narrowest spikes, showed a distinct post-AHP depolarization, or "rebound AHP" (rAHP), lasting nearly 30 ms, and tended to fire at 25–35 Hz. The evidence suggests that an intrinsic rAHP may confer on these neurons a tendency to fire at a preferred frequency governed by the duration of the rAHP and may contribute to a "pacemaking" role in generating cortical oscillations.

INTRODUCTION

The timing of action potentials in cortical neurons is determined by the cells' synaptic input from other neurons and by their intrinsic membrane properties (Llinas 1988). The intrinsic membrane mechanisms of neocortical neurons during steady-state or modulated firing have been characterized extensively in vitro by intracellular recordings in cortical slice preparations, which offer stable recording conditions (Crill 1996; Schwindt and Crill 1999). Neurons recorded in cortical slices of guinea pigs were classified based on their characteristic afterhyperpolarizations (AHPs) and other physiological properties (Connors et al. 1982; McCormick et al. 1985). Similar types of firing patterns have been observed in anesthetized rat cortex in vivo (Pockberger 1991). In cat motor cortex, in vivo recordings have revealed subtypes of neurons based on their firing patterns and their responses to stimulation of the pyramidal tract (Baranyi et al. 1993a,b).

In awake animals, cortical neurons constantly receive a variety of synaptic inputs. Unlike the relatively quiescent intracellular membrane potentials of neurons in brain slices or anesthetized preparations, the membrane potentials of neurons in awake behaving animals exhibit large fluctuations arising from barrages of postsynaptic potentials (PSPs), especially during execution of behavioral tasks (Matsumura 1979). Although the intrinsic firing properties of cortical neurons have been elucidated by numerous in vitro studies, the extent to which these properties are preserved or modified by normal synaptic inputs remains unknown (Bernander et al. 1991). Also unclear are the possible functional roles these intrinsic properties could play and their contribution to generation of the firing patterns observed in vivo. These issues can be addressed only by intracellular recordings from neurons in awake animals performing behavioral tasks. The intrinsic properties can be revealed by the characteristics of membrane potentials after averaging random synaptic fluctuations.

Besides influencing firing patterns, intrinsic neuronal properties may also affect patterns of network activities such as cortical synchrony and rhythmicities. The possible physiological significance of such network activities has generated much investigation and speculation. For instance, the gamma-frequency oscillations that occur in many species (Murthy and Fetz 1996a; Singer 1993; Steriade et al. 1991a, 1996), including humans (Aoki et al. 1999; Llinas and Ribary 1993), have been implicated in behavioral conditions of increased alertness (Bouyer et al. 1981; Murthy and Fetz 1996a,b) and in visual binding (Singer and Gray 1995). In motor cortex of behaving monkeys, robust oscillations at 20–35 Hz occur during exploratory hand movements (Fetz et al. 2000; Murthy and Fetz 1996a,b), during an instructed delay period before movement (Sanes and Donoghue 1993), and during maintenance of a precision grip (Baker et al. 1997). The neuronal mechanisms generating such cortical oscillations remain elusive. Two classes of mechanism have been considered: resonant activity in neuronal circuits and intrinsic pacemaker properties of cortical or subcortical neurons. Studies on both in vivo and in vitro preparations have found rhythmic firing of action potentials that correlated with subthreshold oscillatory membrane potential or intrinsically generated bursts of spikes (Steriade 2001; Traub et al. 1999), and have also implicated intracortical or corticothalamocortical pathways and cortical inhibitory interneurons (Cobb et al. 1995).

To elucidate these issues, we analyzed membrane potentials surrounding the action potentials recorded intracellularly in motor cortical neurons of awake behaving or lightly anesthetized primates. Because variations in firing behavior among cortical neurons could result either from a variation in synaptic inputs or from different intrinsic membrane properties of individual neurons, we used spike-triggered averaging (STA) to eliminate the "synaptic noise" (i.e., the random fluctuations in

Address for reprint requests and other correspondence: D. Chen, National Institute of Neurological Disorders and Stroke, 6001 Executive Blvd., MSC 9523, Bethesda, MD 20892-9523 (E-mail: daofen.chen@nih.gov).

The costs of publication of this article were defrayed in part by the payment of page charges. The article must therefore be hereby marked "*advertisement*" in accordance with 18 U.S.C. Section 1734 solely to indicate this fact.

membrane potentials), to reveal underlying intrinsic membrane potentials. The biophysical tests that can be applied to in vivo study in awake behaving animals are limited, although this approach provides a powerful new tool toward quantitative measurement of the characteristic features of membrane potential trajectories that result from intrinsic properties. We hypothesize that action potentials with distinctive membrane trajectories are associated with specific steady-state firing patterns of motor cortical neurons in awake behaving primates. We found three types of AHPs and three different trajectories of subsequent interspike intervals (ISIs), each with characteristic features. Neurons in one group showed a distinct post-AHP depolarizing rebound ending at about 30 ms after the spike; these neurons all tended to fire at 25–35 Hz. The distinctive trajectory of the ISI membrane potential of these neurons may play a "pacemaking" role, allowing them to fire preferentially at a frequency that correlates with the duration of the AHP. We propose that the activity of these neurons may contribute to the entrainment of sensorimotor cortical networks into episodes of gamma-frequency oscillations.

METHODS

We recorded intracellular membrane potentials and firing activities of neurons in the sensorimotor cortex from eight hemispheres of five chronically prepared macaque monkeys weighing 3.2–6.2 kg (three *Macaca fascicularis* and two *M. nemenstrina*) (Matsumura et al. 1996). Recordings were made with the monkey either under light halothane anesthesia (for four hemispheres) or awake and performing alternating wrist movements in a target-tracking task (Fetz and Cheney 1980).

Surgical preparation

With the monkey deeply anesthetized with Nembutal (Abbott, 3 mg/kg, imp) or halothane, an acrylic stabilizer for semichronic recording was implanted on the skull (Matsumura et al. 1996). The implant contained stainless steel tubes for anchoring the head to a stereotaxic frame mounted on top of the primate chair, where the electrode carriers were placed. Before the recording session, the monkey was given a small dose of ketamine (0.5 mg/kg, intramuscular) and lightly anesthetized with halothane (0.5–1%, with 2–3 L/min oxygen and 1 L/min nitrous oxide), and seated in the primate chair with the head anchored. A small elliptical hole (about 2×3 mm) was drilled through the acrylic and the skull at a site within the area covering the anterior portion of the central gyrus. The dura was incised with a fine needle to expose the surface of the cortex.

Electrophysiological recordings

Intracellular recordings were obtained with glass (OD 2 mm) or quartz (1 mm) micropipettes filled with 2 M K-methylsulfate with resistance between 10 and 40 MΩ. Electrodes were inserted into the cortex with an electrode carrier at an angle of 15–20° from vertical in the parasagittal plane, and advanced by a pulse-stepping microdrive (Burleigh Inchworm). After the electrode tip was placed in the superficial cortical layer, the hole in the skull was filled with 4% agar dissolved in saline to dampen cortical pulsations and to prevent tissue from drying. The animal was allowed to recover from the light anesthesia for ≥30 min. The recording electrode was advanced when the monkey began to perform an isometric wrist flexion–extension task. The electric signals from the IC electrode were amplified to provide both low-gain DC (0–10 kHz) and high-gain AC records (1 Hz to 10 kHz). All signals were recorded at 0- to 5-kHz bandwidth on a 14-channel FM tape recorder (Honeywell 101). The depth of the recorded cell was registered with reference to the cortical surface. At the end of each recording session, the monkey was lightly anesthetized with either ketamine or halothane. To mark the recording sites, DC currents of 10 μA were passed for 10 s through a carbon-fiber electrode inserted next to the intracellular pipette to make coagulated deposits (Sawaguchi et al. 1986). Electrodes were then withdrawn, and the skull opening was treated with topical antibiotics and filled with dental cement. For histology, monkeys were perfused with saline followed by 10% formalin under deep Nembutal anesthesia. The brain was postfixed in 30% sucrose–formalin solution and prepared for 100-μm sections. The recording sites were identified with the location of the surface entry, and the cortical depth was confirmed with the aid of the depth marker on the electrode carrier and detectable carbon deposit in the section.

Spike-triggered averaging and data analysis

To analyze the interspike membrane potential trajectories, intracellular membrane potentials between two consecutive action potentials were averaged from the DC channel (sampling rate of 150 μs) with the use of a Window Discriminator to provide triggers from the action potentials. Two averaging approaches were used, both triggered by intracellular action potentials. For neurons that were held long enough to generate sufficient activity the computer compiled interval-triggered averages (ITAs) by accepting only sweeps in which another action potential fired before the triggering one at the predetermined intervals. This was done for a series of fixed intervals (100, 90, 80, . . . , 65, 60, . . . , 15 ms, etc.) with a ±1-ms acceptance time window for each ISI, producing a set of averages at different intervals for a particular intracellularly recorded cell. For neurons that had short recording time and low firing activities, the averager accepted every sweep that did not have another action potential during 40 ms before and 60 ms after the triggering action potential. Measurements of the features of ISI membrane potential trajectories were made on the averaged traces. The voltage level of firing threshold and the spike onset were determined by the value of the bin just before the one representing the abrupt rising phase of the action potential.

RESULTS

Results were obtained from intracellular recordings from precentral cortex in eight hemispheres of five animals (Matsumura et al. 1996). Most recordings were obtained while the monkeys performed an isometric wrist flexion–extension task. Task-related neurons recorded in the contralateral motor cortex exhibited increased fluctuations of membrane potentials and/or membrane depolarization triggering action potentials during the excitatory phases. We believe that these recordings are mainly somatic because the recording stability in this behavioral preparation would probably be insufficient for sustained dendritic recordings. A chronic multielectrode recording during isometric ramp-and-hold wrist responses is shown in Fig. 1. The intracellularly recorded cell fired action potentials repetitively during wrist-extension torques (downward deflection). The extracellular spike activity recorded simultaneously from neighboring neurons with another electrode also showed weak increases during extension. An expanded segment of the membrane potential trajectories is shown in the *bottom trace*. Typical of the in vivo recordings in awake monkeys, individual trajectories were highly variable, due to the presence of substantial synaptic noise. To reveal underlying features of the membrane potential trajectories we used two averaging techniques (see METHODS). STAs of the pre- and postspike trajectories revealed intrinsic perispike membrane potential profiles,

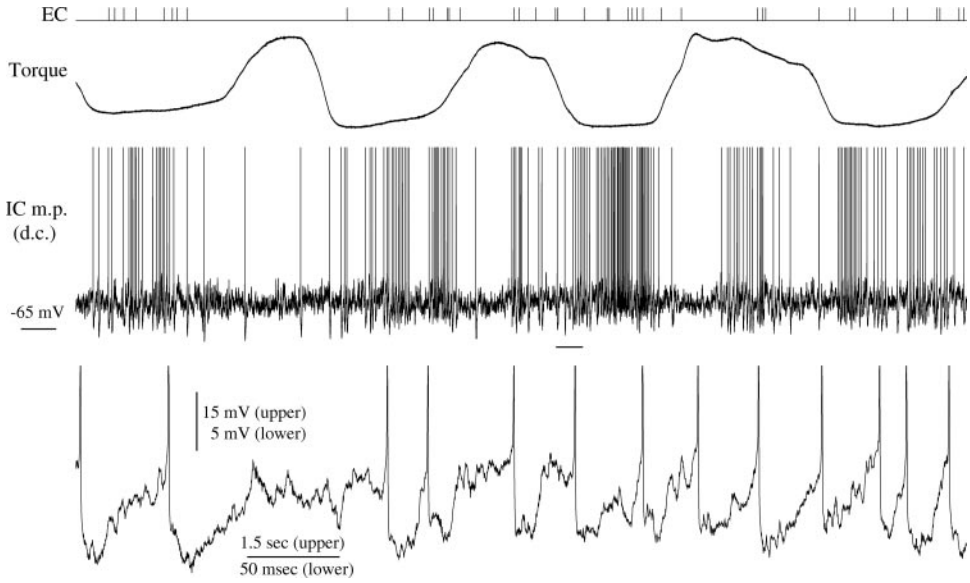

FIG. 1. Simultaneous 2-electrode recordings of spikes from an extracellular unit (EC, shown as acceptance pulses from window discriminator), torque, and intracellular (IC) membrane potential from another neuron. *Bottom trace*: expanded version of the marked section in the *top IC trace*. IC cell was recorded at a cortical depth of 1,760 μm and EC at 1,600 μm in the precentral dimple area of the right hemisphere while monkey C performed the motor task. *Top IC trace* was clipped at −20 mV and the *bottom trace* at −55 mV. Both are DC coupled.

as well as the height and width of the action potentials. ITAs showed the mean membrane potential trajectories in specific ISIs. These averages reduced the synaptic fluctuations and revealed consistent characteristics of the membrane potential trajectories.

All 64 of the intracellularly recorded neurons exhibited stable "resting" membrane potentials of at least −50 mV for the recordings analyzed, overshooting or near-overshooting action potentials, and a wide range of firing rates during spontaneous and task-related activity. They were recorded throughout the cortical layers of the sensorimotor cortex, although most (87%) were in layers below 1,200 μm, corresponding to layer V/VI in primate motor cortex.

Characteristics of three basic types of cortical neurons

The recorded and analyzed neurons were divided into three major groups based on the width of their action potentials, the characteristics of their AHPs, and the trajectories of the subsequent ISIs revealed by the averages. Neurons with different types of AHPs could be recorded with the same electrode in a given track under the same behavioral conditions. Characteristic features of the three types recorded from the motor cortex of an awake monkey are shown in Fig. 2. The most commonly observed neurons were *type I*, which exhibited a "scoop-shaped" AHP (Schwindt et al. 1988b). Their action potentials were relatively wide, measured at half-amplitude from the STA traces: 1.4 ± 0.5 ms, mean ± SD (n = 31; 25 from awake and six from anesthetized monkeys). Amplitudes of these action potentials were 66.2 ± 12.8 mV. All but eight of the 31 neurons were recorded >1,200 mm below the cortical surface. Their initial fast repolarization transitioned gradually to a rounded "scoop-shaped" AHP, followed by a slow, continuous rise to a resting level or the next firing threshold. ISI histograms compiled for 21 type I neurons that fired long enough showed various features. Twelve exhibited wide ISI distributions, with no consistent or distinct peaks; the rest had clear peaks centered at different ISIs. Three showed broad peaks centered at 35–50 ms (Fig. 2*B*, type I).

The *type II* neurons exhibited significant afterdepolarizing potentials (ADPs) of about 1–3 mV after the initial spike repolarization; then, after a small and slow hyperpolarization, membrane potentials rose gradually to the level of subsequent action potentials (Fig. 2, Type II). Their action potentials had a width of 0.7 ± 0.2 ms and an amplitude of 63.2 ± 13.4 mV (n = 17; 16 from awake and one from anesthetized monkeys). All were recorded >1,200 μm below the cortical surface. ISI histogram profiles for these neurons also vary and exhibit no consistent peak features, except that nine of these 17 neurons showed an additional sharp peak at intervals of <10 ms (Fig. 2*B*, Type II), indicating a tendency to fire high-frequency doublets of action potentials. These doublets, however, were sporadic and not repetitive. Histograms for two of the neurons also showed a peak at about 30 ms (Fig. 4). We did not observe any repetitive bursting firing activities when the animals were alert or performing the task; bursts occurred only during anesthetized or drowsy states, and only in alpha frequencies, i.e., <14 Hz.

The most remarkable AHP characteristics were exhibited by *type III* neurons. These cells had narrow action potentials (0.5 ± 0.2 ms) with an amplitude of 53.8 ± 9.6 mV (n = 16, 13 from awake and three from lightly anesthetized monkeys). All but two were recorded below 1,200 μm. Action potentials of type III neurons showed an initial instantaneous repolarization, which deviated to a slower hyperpolarization lasting 5–9 ms, followed by a depolarizing rebound of 20–25 ms to a flat resting level or to a subsequent action potential, as shown in Figs. 2*A* and 5. The abrupt change from a fast to a slower repolarization rate usually occurred at a voltage level close to the resting baseline, i.e., at 5.9 ± 2.7 mV (n = 9) above the bottom of the AHP troughs or 8.4 ± 2.9 mV (n = 9) below the spike threshold. After reaching the bottom of the AHP trough, the membrane potentials exhibited a fast post-AHP depolarizing rebound to the resting baseline and remained at that level until the onset of a prethreshold ramp potential (PTRP) before the next action potentials. We will call AHPs with this distinct rebound depolarizing phase "rebound AHP," or rAHP (Gutnick and Yarom 1989; Llinas and Yarom 1981). The features of this rAHP and the ISI trajectories exhibited by type III neurons are distinctly different from those in the other two groups (cf. Figs. 2–5). Instead of a smooth, continuous transi-

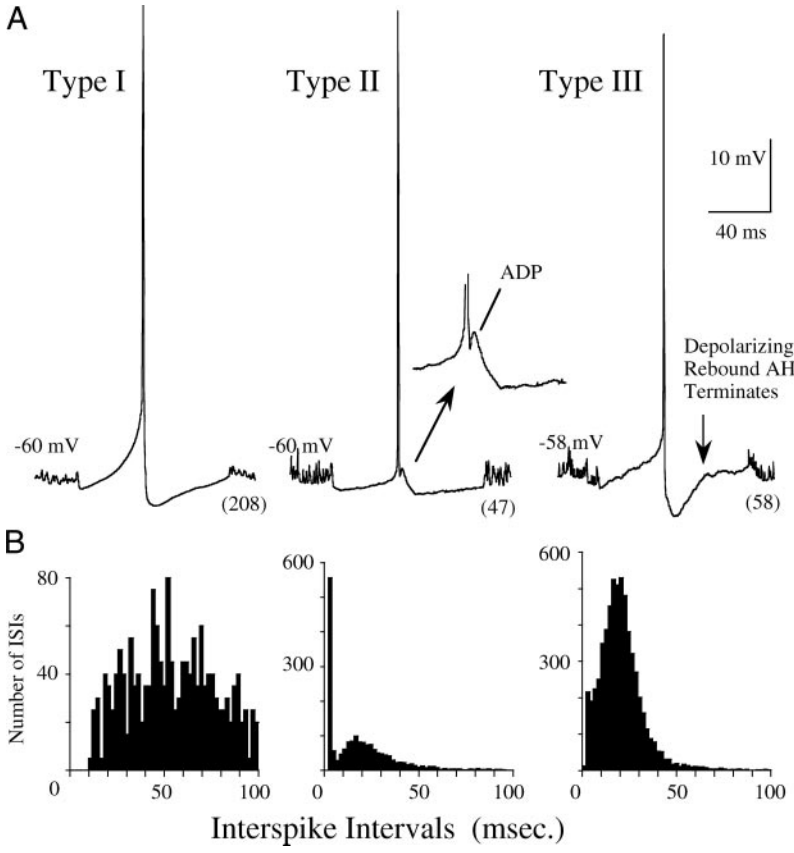

FIG. 2. Representative examples of 3 types of AHPs (*A*) and their interspike interval (ISI) histograms (*B*) recorded from awake monkey E. Each accepted sweep for averaging contained only one action potential, i.e., the triggering spike, in a total range of 100 ms (40 ms pretrigger and 60 ms posttrigger). *Inset* for Type II shows an enlarged view of afterdepolarizing potential (ADP). Voltage level indicated at the *bottom left* in *A* are steady-state "resting" membrane potentials registered on a low-gain DC couple oscilloscope.

tion from the bottom of the AHP to the PTRP of the next action potential, there were two consistently identifiable turning points for ISIs longer than about 35 ms: one occurring when the rebound phase of the AHP transitioned to a relatively straight baseline membrane potential, and the other when the prethreshold rising phase deviated from the baseline (see Fig. 5, *bottom* and *middle* arrows). ISI histograms for 12 type III cells revealed a strong tendency to fire action potentials at frequencies of 22–45 Hz (at a mean ISI histogram peak of 29.9 ± 6.8 ms; cf. Figs. 2*B* and 5).

In eight neurons whose recordings were held long enough (15–40 min), we compiled average ISI trajectories for different depolarization levels (three type I, one type II, and four type III). Changing the membrane potential in the range $< \pm 10$ mV by injecting sustained depolarizing or hyperpolarizing current changed only the firing rate and the relative size of the averaged AHPs; it did not alter the characteristic features of the AHPs and subsequent trajectories for ISIs longer than about 30 ms. Thus the effect of superimposed injected current on averaged trajectories was essentially equivalent to that of synaptically generated current.

Consistency of the descriptive characteristics at different firing frequencies

To examine the characteristics of the AHPs and interspike trajectories in relation to different ISIs, we averaged the membrane potentials for various fixed intervals between pairs of intracellular action potentials. These ITAs were compiled in neurons that showed high spontaneous or task-related activity, providing sufficient number of triggers at various frequencies to attain a set of ITAs for at least five different intervals within the range of 30–100 ms.

TYPE I AHPS. ITAs obtained for a type I neuron recorded in an awake, behaving monkey are shown in Fig. 3. These 12 traces, aligned with the triggering action potentials, show the averaged trajectories of interspike membrane potentials for 12 fixed intervals. The 2-ms acceptance window for each interval selected sweeps that had ISIs within ±1 ms of the specified interval. Ten superimposed ITAs for this cell are also shown at their absolute voltage levels (*top left*).

The ITAs reveal that the scoop shape of the AHPs and the subsequent trajectories were relatively stereotyped, regardless of the ISI duration. The voltage levels between the two action potentials were elevated as the ISIs shortened (see the superimposed display), but the trajectories followed roughly the same paths to merge into the PTRP. The noisy appearance of the pre- and post-ISI traces results from the effect of averaging of the action potentials that occurred at various times in the individual sweeps. The absence of any significant smooth trajectory "hump" before or after these ISIs indicates a lack of particular firing rhythm. The ISI histogram for this neuron (Fig. 3, *top right*) peaked at the shorter intervals and exhibited a broadly distributed interspike intervals.

TYPE II AHPS. ITAs obtained for a type II neuron are shown in Fig. 4. Like other type II neurons, this cell exhibited a consistent afterdepolarizing (ADP) potential after the initial instantaneous repolarization, and a subsequent slow rise of the ISI trajectories. The general shape and relative sizes of these features were consistent for different averaged intervals. Similar to the type I neurons, the ISI trajectories for the type II

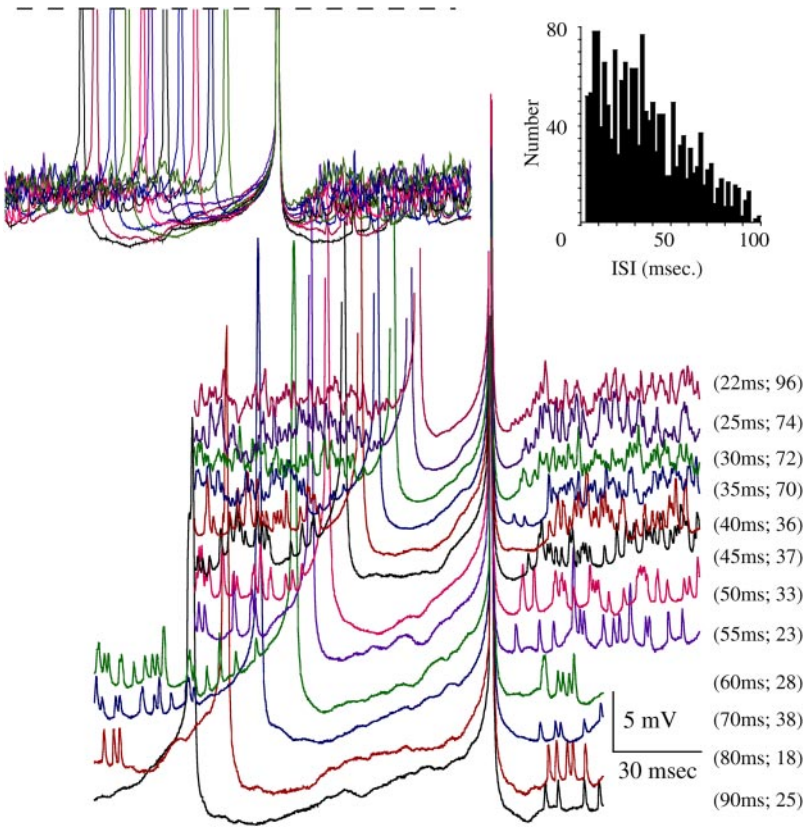

FIG. 3. ISI trajectories of a type I neuron. Cell recorded in the anterior part of the primary motor cortex of an awake monkey. Display of sweeps is stacked for clarity. For each trace the numbers in parentheses give the ISI duration that has been used as acceptance criteria for averaging and the number of sweeps averaged for that trace. Cutoff on the *right* of the *bottom 4 traces* was due to the limit in total sampling points allowed by the averager. ISI histogram for this neuron is shown on the *top right*. *Top left inset*: superimposed display of ISI trajectories aligned at action potential threshold. ISIs were 65, 60, 55, 50, 42, 37, 32, 27, 22, and 17 ms.

followed roughly the same paths to merge continuously and smoothly into the PTRP leading to the firing levels. The ADPs occurred in all the ITAs compiled; for very short intervals they merged directly into the PTRP without any intervening hyperpolarization (see *top trace* for 15-ms ISI). About half of the type II neurons fired occasional high-frequency doublets of action potentials, but none showed *repetitive* bursting activity during the awake behaving state, such as reported for visual cortex (Gray and McCormick 1996). However, unlike the type I neuron in Fig. 3, the averages for the neuron shown in Fig. 4 did reveal a certain degree of periodicity in firing when the triggering intervals were <45 ms. This periodicity, apparent in the depolarizing waves on both sides of the ISI trajectories, is in roughly the same rhythm at each selected averaging interval (note the corresponding delay of the rhythmic post-ISI depolarizing waves as the selected averaging interval was changed from 40- to 50-ms ISIs, marked by two thin arrows). Although the ISI histogram for this neuron shows a narrowly distributed ISI peak at about 38 ms, the periodicity for the pre- and post-ISI depolarizing waves revealed from the averages varies from ISIs of 15 to 100 ms. A lack of a reliable, consistent, and ISI-independent rhythmicity suggested that the cell may be synaptically entrained to fire synchronously with other neurons around a few particular resonant frequencies, rather than reflecting a tendency imposed by its own intrinsic membrane properties.

TYPE III AHPS. ITAs for the cell with task-related activity shown in Fig. 1 are presented in Fig. 5. Comparing the relative smoothness of the averaged interspike trajectories with the variable membrane trajectories in the raw recording confirms the utility of averaging to reveal the underlying intrinsic membrane trajectory. The features of the AHP and subsequent ISI trajectories of this cell were characteristic of type III neurons. The existence of a consistent post-AHP depolarizing rebound is evident in both the ISI trajectories and the post-ISI trajectories, as illustrated in both the stacked and the superimposed (*top left*) ITAs. The general shape of this rAHP and the subsequent ISI trajectory were stereotyped, although for shorter intervals the lowest voltage level of the AHP was more depolarized and occurred earlier. The distinctive feature of rebound is particularly clear in the superimposed ITA display, in contrast with the nonrebound trajectories of other two types (Figs. 3 and 4). Unlike the ISI trajectories of type I and II neurons, the trajectories of type III neurons did not follow the same straight path from the bottom of the AHP to merge into the PTRP. Rather, for ISIs longer than about 35 ms the membrane potential trajectories from the bottom of the AHP to the PTRP make two transitions: initially they depolarized rapidly to the rest level, and then maintained that flat resting level before merging with the onset of the PTRP. As the interval shortened, the transition point between the end of the rebound and the beginning of the flat resting baseline level, as well as that between the resting level and the PTRP, became less distinguishable, and the three regions blended into each other for averages with ISIs of <30 ms (*top* trajectories in Fig. 5). The averaged traces in Fig. 5 also indicate that the neuron exhibited periodic firing (see *top* downward arrows). Unlike the inconsistent periodicity of the type II neuron in Fig. 4, the neuron in Fig. 5 exhibited a reliable rhythmicity of about 30 Hz, which is evident in most of the averaged traces during both pre- and post-ISIs. This reliable, consistent, and ISI-independent periodicity revealed in the averages indicates that the

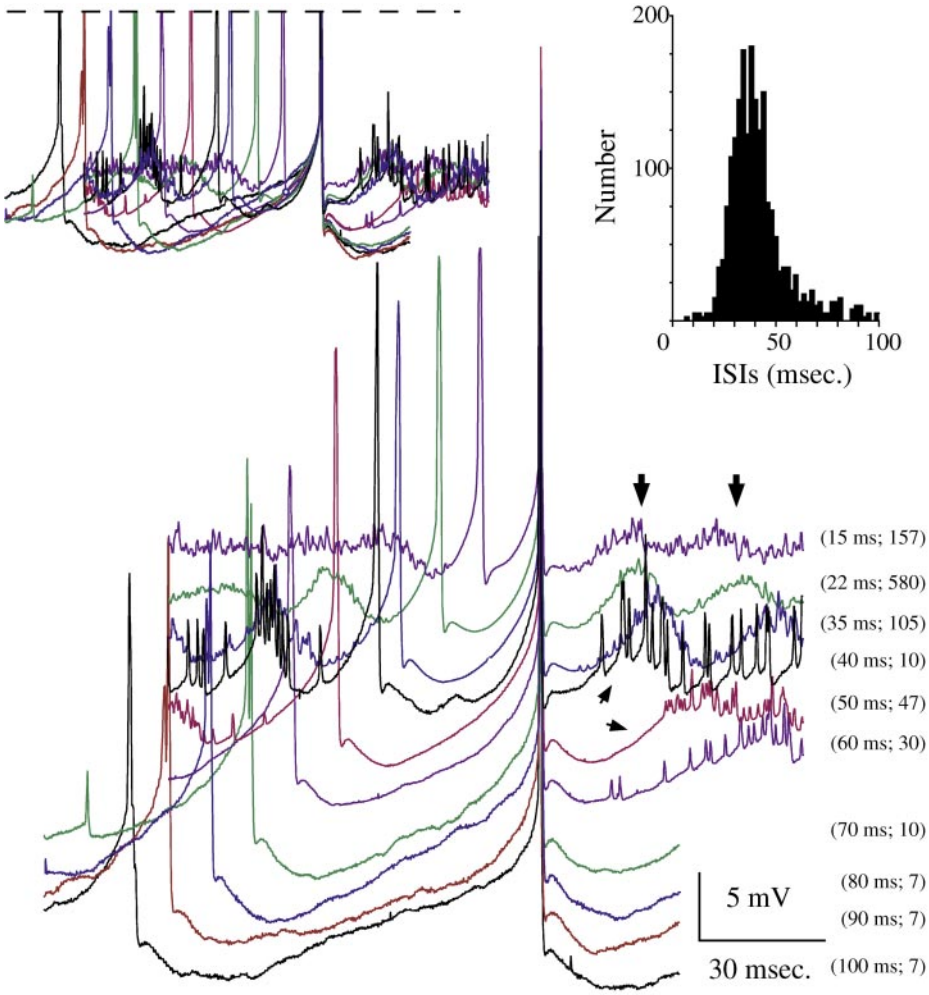

FIG. 4. ISI trajectories of a type II neuron, recorded from an anesthetized monkey. Same trace sets are displayed as stacked and superimposed. Thick arrows indicate the periodic firing activities. Thin arrows indicate the significant difference in the rate of periodic firings between traces with ISIs of ≤40 ms and those ≥50 ms (also seen in the *top left* superimposed display), suggesting that the periodic activities are not explained by the neuron's intrinsic property.

source of the rhythmicity is unlikely to be synaptically entrained. In addition, this periodicity correlated well with the time course of the rebound AHP at each ISI, suggesting that the rAHP conferred a tendency to fire at a preferred frequency governed by the duration of the AHP. For this neuron the average duration of the rAHPs for the longer averaged ISI trajectories (55–100 ms) was about 30 ms. The ISI distribution of this neuron had a clear peak at about 28 ms (histogram in Fig. 5). The ISI histograms of 12 type III cells revealed that the peak values in their ISI histograms correlated well with the mean values of the duration of the rAHP (T_b in Fig. 7*B*) obtained in traces of their averaged trajectories for ISIs >40 ms (Fig. 6, $r = 0.58$, significant at 0.05).

Quantitative measurement and description of the membrane potential trajectories surrounding action potentials with rAHPs

To quantify changes in the characteristic shape of the AHP of type III neurons as a function of the ISIs, we measured the relevant parameters shown in Fig. 7*B*. We documented the absolute voltage level for the action potential firing threshold (V_t) and measured four other voltage levels relative to V_t: the voltage at onset of the PTRP (V_p), the point for transition from the fast to slow repolarization (V_r), the most hyperpolarized level of the AHP (V_h), and the end of the rebound rising phase (V_b). We also measured three time periods: the duration of the PTRP from its onset to spike initiation (T_p), the time of maximal postspike hyperpolarization (T_h), and the duration of AHP (T_b).

Figure 7*A* superimposes the AHP trajectories of the neuron in Fig. 5 to show that as the firing rate increased and ISIs shortened, the voltage levels of the AHPs were continuously elevated—from 12.4 mV below firing threshold at the 65-ms ISI to 8.3 mV at the 15-ms ISI. Likewise, the duration of the slow repolarization (T_h) decreased (from 7.6 ms at the 65-ms ISI to 3.8 ms at the 15-ms ISI). These rate-dependent changes were roughly linear for ISIs ranging from 45 to 15 ms. The absolute voltage levels of firing threshold for this neuron were relatively steady, remaining at about -53.8 ± 1.1 mV for the 15 averaged ISIs. Measurement of the absolute voltage level of firing threshold from sets of averaged ISIs in a total of nine neurons showed that three remained constant, four increased steadily, and two decreased steadily as a function of firing frequency. Their pooled values (V_t) are shown in Fig. 7*C*.

Quantitative measurement of these features was possible for nine of the 16 type III rAHP neurons adequately documented over a sufficient range of frequencies. The parameters for these neurons were grouped for different ISIs, and the means and SDs are plotted in Fig. 7, *C* and *D* as a function of ISI. The voltage drop between spike threshold and the most hyperpo-

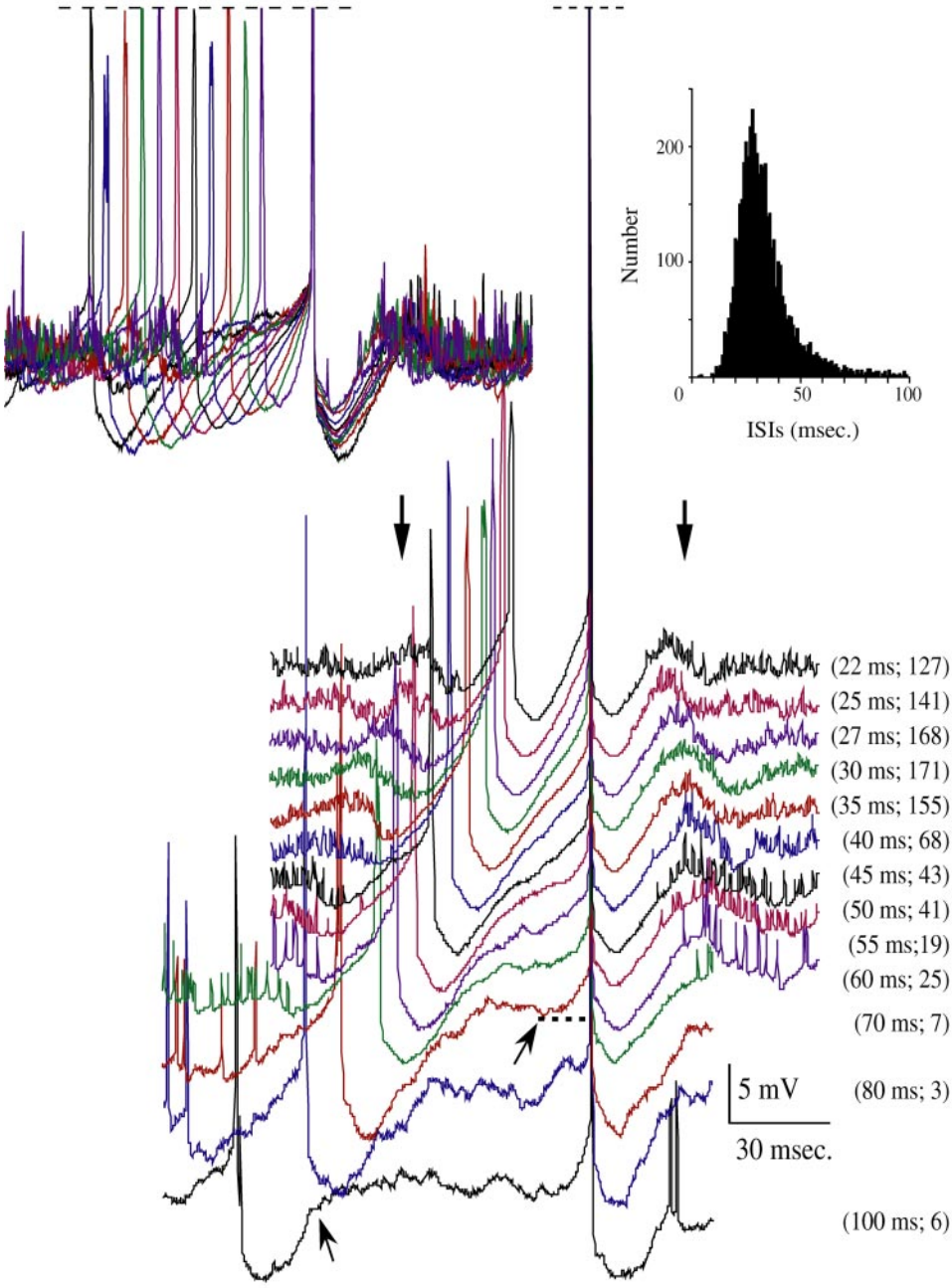

FIG. 5. ISI trajectories of a type III neuron, whose task-related activities are shown in Fig. 1. ISIs and the numbers of the averages for the traces are shown on the *right*. ISI histogram at *top right* shows preference for ISIs at about 30 ms. ISIs for the superimposed display at *top left* were 65, 60, 55, 45, 40, 35, 30, 25, 20, and 15 ms. Two downward arrows indicate the peaks on both sides of the averaged ISIs, resulting from either the subthreshold membrane potential "rebound" from the hyperpolarization or periodic firings at about 30 ms. *Middle* arrow indicates initiation of the prethreshold ramp potential (PTRP). *Bottom* arrow shows the trajectory turning point between the depolarizing phase of the rebound AHP (rAHP) and the "resting" membrane potential.

larized level of AHP, V_h, remained relatively constant for ISIs between 100 and 50 ms, and decreased approximately linearly for ISIs of <45 ms (Fig. 7*C*). Similar changes were seen for other parameters such as V_r (Fig. 7*C*) and T_h (Fig. 7*D*). The measurement of T_b and V_b was limited to ISIs longer than about 40 ms because this transition was difficult to detect as the rising phase of the rebound merged into the rising trajectory to threshold (see Fig. 5). For the measurable range, as the firing frequency increased, the rebound duration decreased slightly whereas V_b remained unchanged. These changes in pooled parameters are representative of most individual cells and suggest that the existence of the rAHPs in these cortical neurons may be attributable to their intrinsic membrane properties (see DISCUSSION). For type III rAHP neurons the onset of a PTRP could be identified for averages with ISIs of >50 ms. For shorter ISIs the end of the rAHP merged smoothly into the

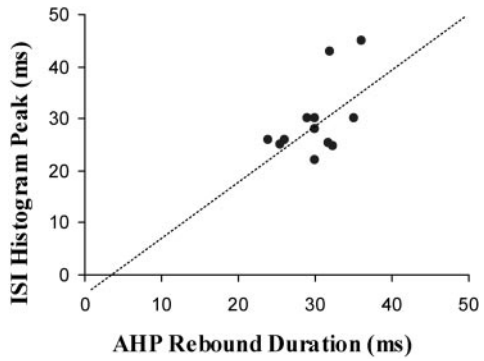

FIG. 6. Relation between averaged duration of the rAHP and peak value of the ISI distribution histogram for 12 type III neurons ($r = 0.58$, significant at 0.05).

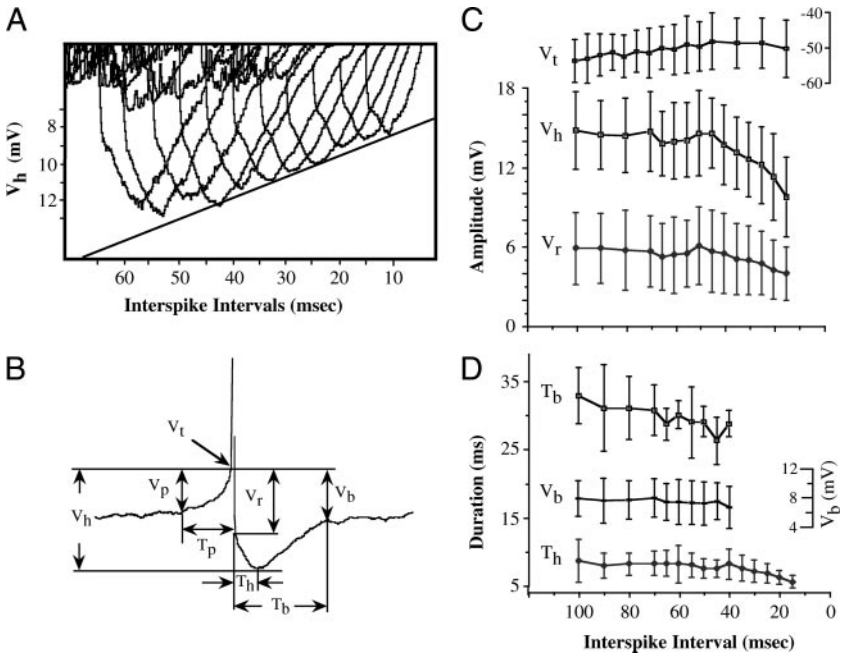

FIG. 7. *A*: enlarged illustration of superimposed average ISI trajectories of type III neuron (same neuron as in Fig. 5), demonstrating graded changes in the duration of the hyperpolarizing phase of rAHP (T_h), and the voltage difference between firing threshold and the most hyperpolarized level of rAHP (V_h). Traces were aligned vertically on the absolute voltage levels for the threshold (V_t). *B*: descriptions for the measurement, made on averaged traces, for features discussed in the text. Voltages measured relative to V_t or the most hyperpolarized level of rAHPs, times measured relative to spike onset or offset. *C*: pooled values measured from 9 Type III neurons for V_t, and amplitude between firing threshold and the most hyperpolarized level of rAHP (V_h) and that of the instantaneous repolarizing phase of rAHP (V_r), as function of ISIs. *D*: reset voltage level (V_b), rAHP duration (Th), and duration of hyperpolarizing phase of the rAHP (T_h), as function of ISIs. Data shown are means ± SD.

prethreshold rising phase (Fig. 5). The voltage deflection marking the onset of the PTRP occurred at a level (V_p) of 8.9 ± 4.6 mV below the threshold (about 2.0 ± 0.8 mV above the baseline), and at a time (T_p) of 8.8 ± 2.0 ms before the threshold. These values did not change systematically with the ISIs. Although similar increases in membrane potential before the action potentials could also be observed for type I and II neurons, they could not be identified and measured reliably and consistently because the ISI trajectories rose continuously and smoothly to the firing threshold.

DISCUSSION

This first analysis of repetitive firings and ISI trajectories of intracellular membrane potentials of motor cortex neurons in awake, behaving primates complements previous in vitro studies. Almost all previous studies have analyzed repetitive firing properties by injecting current into the soma of quiescent cells. All our intracellular potentials were generated by natural synaptic input, presumably generated mainly by dendritic depolarization, which may have different effects on repetitive firing than somatic depolarization (Schwindt and Crill 1999). Under these normal in vivo conditions all cortical neurons showed substantial fluctuations in membrane potentials and timing of action potentials. Averaging the membrane potentials for specific ISIs reduced synaptic noise and revealed three distinguishable groups of stereotyped AHPs and ISI trajectories that characterized cells over a range of firing frequencies. One group of neurons showed a distinct rAHP lasting about 30 ms, followed by a flat trajectory for long ISIs, and these all tended to fire at 25–35 Hz. This suggests that some cortical neurons in awake primates have a distinctive interspike membrane potential trajectory that may confer a pacemaking tendency at these frequencies.

Classification of cortical neurons

To the extent that our cell types correspond to those classified in different preparations it may be possible to make inferences from complementary data sets. Extensive information about the firing characteristics and spike trajectories of cortical neurons has come from studies on slices of rodent cortex. Rat cortical neurons have been classified into fast-spiking, regular-spiking, and intrinsically bursting cells, according to the characteristics of their AHPs and other electrophysiological properties (Connors et al. 1982; McCormick et al. 1985). In an in vivo study of electrophysiological and morphological properties of neurons in the rat motor cortex, Pockberger et al. (1991) also found three types of neurons: *1*) pyramidal cells with moderate firing rate; *2*) bursting small pyramidal neurons or spiny star cells; and *3*) small aspiny cells with radial dendritic field and high firing rate, presumably local inhibitory interneurons. Neurons in the cat sensorimotor cortex also have been classified on the basis of their morphological and electrophysiological characteristics (Baranyi et al. 1993a; Chen et al. 1996a; Dykes et al. 1988; Landry et al. 1984; Spain et al. 1991a; Woody and Gruen 1978). In anesthetized cats Baranyi et al. (1993a) distinguished four types of motor cortex cells: regular-spiking and fast-spiking neurons, and two types of bursting neurons, inactivating and noninactivating.

Similar in vitro studies of human cortical tissue excised around epileptic sites confirmed the presence of the regular- and fast-spiking neurons, and discovered a third group with a voltage-dependent shift in firing behavior (Lorenzon and Foehring 1992). In contrast to data from rodents and cats, no intrinsic burst-firing neuron was observed in human association cortex (Foehring et al. 1991).

The three groups of neurons described in our study were classified entirely on the basis of intrinsic physiological properties, i.e., the spike width and the trajectory features of the ISI-triggered averages of AHPs under normal conditions. Many of the testing criteria used in in vitro studies on relatively quiescent neurons could not be reproduced routinely in our recording condition. Thus we have no morphological correlates for our three groups because systematic intracellular staining and reconstruction were impractical in this preparation. In rodents, slowly adapting or nonadapting neurons with ex-

tremely narrow action potentials were identified as sparsely spiny nonpyramidal inhibitory (GABAergic) interneurons (McCormick et al. 1985), but in cat motor cortex, large layer V pyramidal cells also had very thin spikes (Dykes et al. 1988).

Recent in vivo studies suggested that the distinctions between the intrinsic electrophysiological properties of neocortical cell classes are more labile than conventionally thought (Steriade et al. 1998). The membrane and firing properties of neurons may change as a function of different physiological states, such as levels of alertness. Transformations between different firing patterns have been demonstrated during arousal elicited by stimulating the brain stem reticular formation in vivo (Steriade et al. 1993a) or activating receptors with muscarine or glutamate in vitro (Wang and McCormick 1993). We have not observed any neurons that switched from one type of AHP to another under our behavioral conditions.

Mechanisms of rhythmic bursting

The intrinsically bursting neurons in slices of rat cortex often exhibit prominent ADPs [or depolarizing afterpotentials (DAP), a term used to describe the same characteristic (e.g., Baranyi et al. 1993a; Tseng and Prince 1993) when they fire in individual spike mode (Connors and Gutnick 1990)]. With prolonged depolarization, many of these neurons can generate rhythmic bursts in the range of 5–15 Hz (Agmon and Connors 1989; Silva et al. 1991; Tseng and Prince 1993). An in vitro study on cat sensorimotor cortex linked the burst-spiking with the prominent ADP of the recorded neurons, and found the bursting neurons to be in layers II, III, and V and morphologically indistinguishable from regular-spiking neurons (Nishimura et al. 1996). In barbiturate-anesthetized cats, bursts with doublets or triplets could be elicited to fire rhythmically at 20–30 Hz in fast pyramidal tract neurons (PTNs) by a step of injected current (Calvin and Sypert 1976). As mentioned, two subgroups of bursting neurons, inactivating and noninactivating, have been described in the motor cortex of awake cats, with the former mostly identified as either slow PTNs or non-PTNs with a more prominent ADP after the action potential and the latter as either fast PTNs or non-PTNs (Baranyi et al. 1993a). Recent in vivo studies on anesthetized cats have found rhythmic bursting activities with multiple within-burst action potentials stemming from ADPs in corticothalamic neurons of motor and association areas (Steriade et al. 1998) and in pyramidal neurons in striate cortex (Gray and McCormick 1996).

Extracellularly recorded bursting firing patterns have been reported in the motor cortex and middle temporal visual area of behaving monkeys (Bair et al. 1994; Taira and Georgopoulos 1993). Although half of our type II ADP-type neurons fired infrequent doublets, we observed rhythmic burst firing superimposed on large depolarizing waves in alpha frequency only when the animal was drowsy. These differences may be related to species, cortical area, or behavioral state.

Synaptic mechanisms underlying rAHP

The features of the averaged AHPs and ISI trajectories were remarkably stereotyped and stable during the entire course of recordings for almost all the cells analyzed. In accordance with previous studies (Schwindt et al. 1988a; Spain et al. 1991a,b), we interpret the characteristics of these AHP features as reflecting properties of intrinsic membrane conductances. Of particular interest are the rAHP trajectories of the type III neurons, which tended to fire at 30 Hz. An alternative mechanism for generating this rAHP would be synaptic potentials produced by cortical networks. Several observations make this explanation unlikely.

First, the trajectory averages of these neurons are not characteristic of STAs from cells entrained with cortical oscillations (Chen 1993; Matsumura et al. 1996). When spikes became synchronized with local field potential (LFP) oscillations, STAs showed the triggering action potential riding on a broad depolarization wave coincident with the LFP negativity, usually with additional oscillations in the membrane potentials. The duration of this depolarizing wave was typically about 15 ms, in accordance with the periodicity of entrained spikes (Murthy and Fetz 1996b). Records of this type were excluded here and will be described separately. In contrast, the ITAs of type III cells for long ISIs show the characteristic rAHP after both spikes, but no periodic fluctuations in the intervening membrane potential (see *lowest traces* in Fig. 5). Moreover, the same stereotyped AHP appeared for all ISIs longer than about 30 ms, independently of firing frequency. These observations are inconsistent with the hypothesis that the rAHP is generated by oscillatory synaptic inputs, but are readily consistent with an intrinsic spike-dependent mechanism.

Second, the possibility of any recurrent or synchronized PSPs, caused either through chemical synapse or electrotonic coupling, can also be excluded. The rAHP amplitudes were several millivolts, whereas recurrent EPSPs are only several hundred microvolts (Kang et al. 1988; Matsumura et al. 1996). The possibility of a coactivation by electrically coupled cortical neurons is unlikely due to the low coupling ratio (about 10%) and a relatively depolarized reversal potential (−53 mV) (Galarreta and Hestrin 1999; Gibson et al. 1999; Tamas et al. 2000). Even the amplitudes of the averaged compound PSPs triggered by LFP cycles were usually <1 mV (Chen 1993; Penttonen et al. 1998). Furthermore, many IC cells exhibited no rAHP, despite the presence of large rhythmic membrane depolarization in some of the averaged traces before and after the triggering interval (e.g., the type II cell in Fig. 4).

Finally, the consistency of the averaged shape of the rAHPs over a range of intervals and the consistent systematic changes in the parameters of the slow repolarizing phase (V_h, V_r, and T_h) argue against a time-locked synchronized synaptic input. If the rAHP were caused by a postspike inhibitory postsynaptic potential (IPSP), its amplitude would increase with the depolarization associated with increased firing; instead, the AHP amplitude decreased. Nor is the depolarizing rebound likely attributable to a delayed EPSP because this would require a circuit reliably delivering the EPSP 30 ms after each spike. In contrast to contrived circuit mechanisms, the consistent changes in the rAHP as the membrane potentials depolarize with increasing firing rate are readily explained by the behavior of voltage-sensitive ionic conductances.

Conductance mechanisms underlying rAHP

AHPs reflect changes in active ionic conductances after action potentials (Llinas 1988; Schwindt et al. 1988a, 1992). Conductance changes for AHP shapes similar to those de-

scribed here have been documented in in vitro recordings of Betz cells in cats and humans (Chen et al. 1996a,b; Foehring et al. 1989, 1991; Spain et al. 1991b). Trajectories similar to our rAHPs were categorized as medium AHP (mAHP) in cats, where amplitudes of 2–4 mV and durations of 40–50 ms were recorded after single action potentials (Foehring et al. 1989; Schwindt et al. 1988a,b; Spain et al. 1991a).

Several types of ionic conductance may underlie the generation of the rebound-shaped mAHPs. A fast transient potassium current that inactivates and decays within 20 ms is thought to be responsible for the fast repolarization and initial part of the following hyperpolarization (Spain et al. 1991b). Voltage-clamp experiments revealed two outward currents to be responsible for the short duration and small amplitude of the narrow action potentials in interneurons and some layer V pyramidal cells (Chen et al. 1996b; Spain et al. 1991a). The hyperpolarizing trough of the mAHP may also be mediated in part by an apamin-sensitive calcium-activated potassium current (Schwindt et al. 1988a).

Neurons in slices of mammalian cortex display several currents that could be responsible for generating the depolarizing rebound phase after the hyperpolarization. The nonspecific cation current, I_h or I_{AR}, can be activated by hyperpolarization beyond about −50 mV, does not inactivate, depolarizes the cell toward its equilibrium potential of about −30 mV, and gives rise to the rebound phase of the AHP (Lorenzon and Foehring 1992; Luthi and McCormick 1998; Pape 1996; Schwindt et al. 1992; Spain et al. 1987, 1991a). The hyperpolarization also could deinactivate a low-threshold T-type Ca conductance, contributing to a rebound excitation (Friedman and Gutnick 1987; Huguenard 1996; Sutor and Zieglgansberger 1987).

Cortical neurons with a large component of fast-transient K^+ current also have a high I_h current, narrow spike width, and lower input resistance (Chen et al. 1996b; Spain et al. 1991a). These cells usually have large somas and display posthyperpolarization excitation properties. Similarly, all of our type III cells had narrow action potentials and tended to fire at the end of the rAHP. The fast-transient K^+ current displayed a clear voltage dependency of both its activation and inactivation kinetics, which is consistent with the gradual changes in duration and amplitude of the first half of the trough of our rAHP as the ISIs shortened. The high-frequency firing during spontaneous or task-related activity was usually associated with a larger depolarization of membrane potentials, and this may have inactivated the fast-transient K^+ current, leading to smaller and shorter hyperpolarizations (Stafstrom et al. 1984a).

Conductances with a possible role in the rebound [i.e., I_h, T-type Ca, and $I_{K(A)}$] all require hyperpolarization below −50 mV in in vitro preparations for either activation (I_h) (Pape 1996) or deinactivation [T-type Ca and $I_{K(A)}$] (Connor and Stevens 1971; Friedman and Gutnick 1987; Spain 1991a). This corresponds to the steady-state resting membrane potentials we registered for most of our cells. The membrane potential fluctuations of these neurons included transient or sustained hyperpolarizations several millivolts beyond what is required for activation or deinactivation of those conductances. Further information is clearly desirable about the activation properties of these conductances in vivo for motor cortex neurons.

rAHP as a pacemaker for gamma rhythm

The intrinsic tendency of our type III cells to fire at 25–35 Hz may contribute to the generation of gamma-frequency cortical rhythmic activities, which have been suggested to be associated with general alertness (Murthy and Fetz 1992; Steriade et al. 1991a) and cognitive processes (Singer 1993). Because intracortical synaptic transmission between neurons can be unreliable, especially for distances beyond about 500 μm, arising from the paucity of synaptic contacts (Gil et al. 1999; Kisvarday et al. 1986) and the low probability of release (Matsumura et al. 1996; Stevens and Wang 1995; Thomson et al. 1993), it has been proposed that transmission can be made reliable by synchronous convergent inputs from multiple sources (Diesmann et al. 1999) and that an intrinsic rhythmic pacemaker could allow such convergence to be more precise in time (Lisman 1997). Indeed, in vitro studies have provided evidence that intrinsic membrane properties could support rhythmic firing (Alonso and Garcia-Austt 1987; Berman et al. 1989; Llinas 1988; Schwindt et al. 1988a; Silva et al. 1991).

Gray and McCormick (1996) described a class of pyramidal neurons called "chattering cells," in cat striate cortex. With appropriate depolarization, many of these neurons discharged high-frequency spike bursts (300–600 Hz) that recurred rhythmically between 20 and 70 Hz in response to visual stimulation or current pulses. Because burst rate was proportional to the injected depolarizing current, such bursting was suggested to be an intrinsic firing property. Similar gamma-frequency chattering firing behavior has been described in corticothalamic neurons of cat motor and association areas in vivo (Steriade et al. 1998). The burst firings of the chattering cell are believed to act as a robust pacemaker for 40-Hz oscillation in visual cortex and to provide a reliable signal through short-term facilitation across sparse synapses (Wang 1999). Our recordings from the motor cortex of awake primates did not reveal bursting firings in single cells as fast as the chattering activity described in the visual cortex, even during periods of 30-Hz oscillatory activity. Almost all of our neurons that fired repetitively at gamma-frequency behaved like a beating pacemaker, rather than a bursting one (Stafstrom et al. 1984b).

Despite the lack of detailed morphological information about our recorded neurons, the type III neurons with rAHP are likely to have large somas. In the cat narrow spikes could be generated by both inhibitory nonpyramidal interneurons and by some large layer V pyramidal cells (Chen et al. 1996b; Spain et al. 1991a). Most of the fast-spiking neurons in rodents were GABAergic and evoked IPSPs in neighboring cells (McCormick et al. 1985). Both computational and experimental studies suggest that synchronous oscillations can be generated by networks of cortical inhibitory interneurons (Lytton and Sejnowski 1991; Rinzel et al. 1998). Recent in vitro studies further suggest that synchronous rhythmic activities could be mediated by inhibitory, GABAergic interneurons that are interconnected by chemical and electrical synapses (Beierlein et al. 2000; Benardo 1997; Buzsaki and Chrobak 1995; Fisahn et al. 1998; Galarreta and Hestrin 1999; Gibson et al. 1999; Tamas et al. 2000). These interneurons exhibit a diversity of electrophysiological–anatomical subclasses (Gupta et al. 2000). Many of these chemically or electrically coupled inhibitory interneurons in rat cortex were fast-spiking cells (Gibson et al. 1999), and some had AHPs similar to the rAHPs documented in this study

(see Fig. 3*A* in Tamas et al. 2000 and Fig. 5 in Gupta et al. 2000).

Whether they are excitatory or inhibitory, our type III cortical neurons tended to fire action potentials at consistent intervals, and could thus play a pacemaker role enhancing the synchronous oscillations in primate sensorimotor cortex at frequencies ranging from 20 to 40 Hz. The existence of such neurons in the primary motor cortex of an awake behaving monkey was recently deduced through a computational analysis of extracellular spike trains: for some neurons a transform of the interspike interval histogram yielded a calculated postspike distance-to-threshold trajectory resembling the ISI of our type III neurons (Wetmore and Baker 2003). Under appropriate conditions the intrinsic propensity of these neurons to fire rhythmically would generate periodic synaptic potential that could entrain a larger fraction of the local population into coordinated oscillatory activity (Bush and Douglass 1991; Llinas and Yarom 1981).

Functional role of neurons with rAHP

Assuming that our type III neurons in awake monkeys have intrinsic membrane currents like those documented for the mAHP of the Betz cells in cat neocortex, it remains to consider the functional consequences for the possible behavioral roles of oscillatory activity. The hypothesis that oscillations facilitate associations would give type III neurons a special role in propagating activity through neuronal networks. This function would predict that these cells are preferentially recruited during associative activity. Another hypothesis, that oscillations reflect attentional mechanisms, would predict that the type III neurons are particularly activated and entrain other neurons under the influence of arousing mechanisms. Indeed, the parameters of the rAHP may be appropriately modified by modulation of transmitters (Brumberg et al. 2000; Lorenzon and Foehring 1992; Steriade et al. 1993b). The brain stem cholinergic ascending system has been implicated in cortically induced synchronization and changes in neuronal firing pattern during sleep–wake cycles (Steriade et al. 1991b). Modulation of spike AHP also has been observed in conjunction with reception of reward-related hypothalamic signals by neurons in the motor cortex (Aou et al. 1988). We could not explore these issues in our experiments, but they are amenable to investigation under appropriate behavioral conditions.

ACKNOWLEDGMENTS

We thank Dr. Michikazu Matsumura for help in collecting some of the data, and Drs. P. C. Schwindt and R. C. Foehring for comments on the manuscript. We also thank J. Galid and L. Shupe for technical assistance.

GRANTS

This work was supported by National Institutes of Health Grants NS-12542 and RR-00166.

REFERENCES

Agmon A and Connors BW. Repetitive burst-firing neurons in the deep layers of mouse somatosensory cortex. *Neurosci Lett* 99: 137–141, 1989.

Alonso A and Garcia-Austt E. Neuronal sources of theta rhythm in the entorhinal cortex of the rat. II. Phase relations between unit discharges and theta field potentials. *Exp Brain Res* 67: 502–509, 1987.

Aoki F, Fetz EE, Shupe L, Lettich E, and Ojemann GA. Increased gamma-range activity in human sensorimotor cortex during performance of visuomotor tasks. *Clin Neurophysiol* 110: 524–537, 1999.

Aou S, Oomura Y, Woody CD, and Nishino H. Effects of behaviorally rewarding hypothalamic electrical stimulation on intracellularly recorded neuronal activity in the motor cortex of awake monkeys. *Brain Res* 439: 31–38, 1988.

Bair W, Koch C, Newsome W, and Britten K. Power spectrum analysis of bursting cells in area MT in the behaving monkey. *J Neurosci* 14: 2870–2892, 1994.

Baker SN, Olivier E, and Lemon RN. Coherent oscillations in monkey motor cortex and hand muscle EMG show task-dependent modulation. *J Physiol* 501: 225–241, 1997.

Baranyi A, Szente MB, and Woody CD. Electrophysiological characterization of different types of neurons recorded in vivo in the motor cortex of the cat. I. Patterns of firing activity and synaptic responses. *J Neurophysiol* 69: 1850–1864, 1993a.

Baranyi A, Szente MB, and Woody CD. Electrophysiological characterization of different types of neurons recorded in vivo in the motor cortex of the cat. II. Membrane parameters, action potentials, current-induced voltage responses, and electrotonic structures. *J Neurophysiol* 69: 1–15, 1993b.

Beierlein M, Gibson JR, and Connors BW. A network of electrically coupled interneurons drives synchronized inhibition in neocortex. *Nat Neurosci* 3: 904–910, 2000.

Benardo LS. Recruitment of GABAergic inhibition and synchronization of inhibitory interneurons in rat neocortex. *J Neurophysiol* 77: 3134–3144, 1997.

Berman NJ, Bush PC, and Douglas RJ. Adaptation and bursting in neocortical neurones may be controlled by a single fast potassium conductance. *Q J Exp Physiol* 74: 223–226, 1989.

Bernander NJ, Douglas RJ, Martin KA, and Koch C. Synaptic background activity influences spatiotemporal integration in single pyramidal cells. *Proc Natl Acad Sci USA* 88: 11569–11573, 1991.

Bouyer JJ, Montaron MF, and Rougeul A. Fast fronto-parietal rhythms during combined focused attentive behaviour and immobility in cat: cortical and thalamic localizations. *Electroencephalogr Clin Neurophysiol* 51: 244–252, 1981.

Brumberg JC, Nowak LG, and McCormick DA. Ionic mechanisms underlying repetitive high-frequency burst firing in supragranular cortical neurons. *J Neurosci* 20: 4829–4843, 2000.

Bush PC and Douglass RJ. Synchronization of bursting action potential discharge in a model network of neocortical neurons. *Neural Comput* 3: 19–30, 1991.

Buzsaki G and Chrobak JJ. Temporal structure in spatially organized neuronal ensembles: a role for interneuronal networks. *Curr Opin Neurobiol* 5: 504–510, 1995.

Calvin WH and Sypert GW. Fast and slow pyramidal tract neurons: an intracellular analysis of their contrasting repetitive firing properties in the cat. *J Neurophysiol* 39: 420–434, 1976.

Chen D-F. *Synaptic Interactions Between Primate Cortical Neurons Revealed by In Vivo Intracellular Potentials* (PhD Dissertation). Seattle, WA: University of Washington, 1993, p. 102.

Chen W, Zhang JJ, Hu GY, and Wu CP. Electrophysiological and morphological properties of pyramidal and nonpyramidal neurons in the cat motor cortex in vitro. *Neurosci* 73: 39–55, 1996a.

Chen W, Zhang JJ, Hu GY, and Wu CP. Different mechanisms underlying the repolarization of narrow and wide action potentials in pyramidal cells and interneurons of cat motor cortex. *Neuroscience* 73: 57–68, 1996b.

Cobb SR, Buhl EH, Halasy K, Paulsen O, and Somogyi P. Synchronization of neuronal activity in hippocampus by individual GABAergic interneurons. *Nature* 378: 75–78, 1995.

Connor JA and Stevens CF. Prediction of repetitive firing behaviour from voltage clamp data on an isolated neurone soma. *J Physiol* 213: 31–53, 1971.

Connors BW and Gutnick MJ. Intrinsic firing patterns of diverse neocortical neurons. *Trends Neurosci* 13: 99–104, 1990.

Connors BW, Gutnick MJ, and Prince DA. Electrophysiological properties of neocortical neurons in vitro. *J Neurophysiol* 48: 1302–1320, 1982.

Crill WE. Persistent sodium current in mammalian central neurons. *Annu Rev Physiol* 58: 349–362, 1996.

Diesmann M, Gewaltig M-O, and Aertsen A. Stable propagation of synchronous spiking in cortical neural networks. *Nature* 402: 529–533, 1999.

Dykes RW, Lamour Y, Diadori P, Landry P, and Dutar P. Somatosensory cortical neurons with an identifiable electrophysiological signature. *Brain Res* 441: 45–58, 1988.

Fetz EE, Chen D, Murthy VN, and Matsumura M. Synaptic interactions mediating synchrony and oscillations in sensorimotor cortex. *J Physiol* (*Paris*) 94: 323–331, 2000.

Fetz EE and Cheney PD. Postspike facilitation of forelimb muscle activity by primate corticomotoneuronal cells. *J Neurophysiol* 44: 751–772, 1980.

Fisahn A, Pike FG, Buhl EH, and Paulsen O. Cholinergic induction of network oscillations at 40 Hz in the hippocampus *in vitro*. *Nature* 394: 186–189, 1998.

Foehring RC, Lorenzon NM, Herron P, and Wilson CJ. Correlation of physiologically and morphologically identified neuronal types in human association cortex in vitro. *J Neurophysiol* 66: 1825–1837, 1991.

Foehring RC, Schwindt PC, and Crill WE. Norepinephrine selectively reduces slow Ca^{2+}- and Na^{+}-mediated K^{+} currents in cat neocortical neurons. *J Neurophysiol* 61: 245–256, 1989.

Friedman A and Gutnick MJ. Low-threshold calcium electrogenesis in neocortical neurons. *Neurosci Lett* 81: 117–122, 1987.

Galarreta M and Hestrin S. A network of fast-spiking cells in the neocortex connected by electrical synapses. *Nature* 402: 72–75, 1999.

Gibson JR, Beierlein M, and Connors BW. Two networks of electrically coupled inhibitory neurons in neocortex. *Nature* 402: 75–79, 1999.

Gil Z, Connors BW, and Amitai Y. Efficacy of thalamocortical and intracortical synaptic connections: quanta, innervation, and reliability. *Neuron* 23: 385–397, 1999.

Gray CM and McCormick DA. Chattering cells: superficial pyramidal neurons contributing to the generation of synchronous oscillations in the visual cortex. *Science* 274: 109–113, 1996.

Gupta A, Wang Y, and Markram H. Organizing principles for a diversity of GABAergic interneurons and synapses in the neocortex. *Science* 287: 273–278, 2000.

Gutnick MJ and Yarom Y. Low threshold calcium spikes, intrinsic neuronal oscillations and rhythm generation in the CNS. *J Neurosci Methods* 28: 93–99, 1989.

Huguenard JR. Low-threshold calcium currents in central nervous system neurons. *Annu Rev Physiol* 58: 329–348, 1996.

Kang Y, Endo K, and Araki T. Excitatory synaptic actions between pairs of neighboring pyramidal tract cells in the motor cortex. *J Neurophysiol* 59: 636–647, 1988.

Kisvarday ZF, Martin KA, Freund TF, Magloczky Z, Whitteridge D, and Somogyi P. Synaptic targets of HRP-filled layer III pyramidal cells in the cat striate cortex. *Exp Brain Res* 64: 541–552, 1986.

Landry P, Wilson CJ, and Kitai ST. Morphological and electrophysiological characteristics of pyramidal tract neurons in the rat. *Exp Brain Res* 57: 177–190, 1984.

Lisman JE. Bursts as a unit of neural information: making unreliable synapses reliable. *Trends Neurosci* 20: 38–43, 1997.

Llinas R and Ribary U. Coherent 40-Hz oscillation characterizes dream state in humans. *Proc Natl Acad Sci USA* 90: 2078–2081, 1993.

Llinas R and Yarom Y. Electrophysiology of mammalian inferior olivary neurons *in vitro.* Different types of voltage-dependent ionic conductances. *J Physiol* 315: 549–567, 1981.

Llinas RR. The intrinsic electrophysiological properties of mammalian neurons: insights into central nervous system function. *Science* 242: 1654–1664, 1988.

Lorenzon NM and Foehring RC. Relationship between repetitive firing and afterhyperpolarizations in human neocortical neurons. *J Neurophysiol* 67: 350–363, 1992.

Luthi A and McCormick DA. H-current: properties of a neuronal and network pacemaker. *Neuron* 21: 9–12, 1998.

Lytton WW and Sejnowski TJ. Simulations of cortical pyramidal neurons synchronized by inhibitory interneurons. *J Neurophysiol* 66: 1059–1079, 1991.

Matsumura M. Intracellular synaptic potentials of primate motor cortex neurons during voluntary movement. *Brain Res* 163: 33–48, 1979.

Matsumura M, Chen D, Sawaguchi T, Kubota K, and Fetz EE. Synaptic interactions between primate precentral cortex neurons revealed by spike-triggered averaging of intracellular membrane potentials *in vivo. J Neurosci* 16: 7757–7767, 1996.

McCormick DA, Connors BW, Lighthall JW, and Prince DA. Comparative electrophysiology of pyramidal and sparsely spiny stellate neurons of the neocortex. *J Neurophysiol* 54: 782–806, 1985.

Murthy VN and Fetz EE. Coherent 25- to 35-Hz oscillations in the sensorimotor cortex of awake behaving monkeys. *Proc Natl Acad Sci USA* 89: 5670–5674, 1992.

Murthy VN and Fetz EE. Oscillatory activity in sensorimotor cortex of awake monkeys: synchronization of local field potentials and relation to behavior. *J Neurophysiol* 76: 3949–3967, 1996a.

Murthy VN and Fetz EE. Synchronization of neurons during local field potential oscillations in sensorimotor cortex of awake monkeys. *J Neurophysiol* 76: 3968–3982, 1996b.

Nishimura Y, Kitagawa H, Saitoh K, Asahi M, Itoh K, Yoshioka K, Asahara T, Tanaka T, and Yamamoto T. The burst firing in the layer III and V pyramidal neurons of the cat sensorimotor cortex in vitro. *Brain Res* 727: 212–216, 1996.

Pape H-C. Queer current and pacemaker: the hyperpolarization-activated cation current in neurons. *Annu Rev Physiol* 58: 299–327, 1996.

Penttonen M, Kamondi A, Acsady L, and Buzsaki G. Gamma frequency oscillation in the hippocampus of the rat: intracellular analysis in vivo. *Eur J Neurosci* 10: 718–728, 1998.

Pockberger H. Electrophysiological and morphological properties of rat motor cortex neurons in vivo. *Brain Res* 539: 181–190, 1991.

Rinzel J, Terman D, Wang X, and Ermentrout B. Propagating activity patterns in large-scale inhibitory neuronal networks. *Science* 279: 1351–1355, 1998.

Sanes JN and Donoghue JP. Oscillations in local field potentials of the primate motor cortex during voluntary movement. *Proc Natl Acad Sci USA* 90: 4470–4474, 1993.

Sawaguchi T, Matsumura M, and Kubota K. Long-lasting marks of extracellularly recorded sites by carbon fiber glass micropipettes in the frontal cortex of chronic monkeys. *J Neurosci Methods* 15: 341–348, 1986.

Schwindt P and Crill W. Mechanisms underlying burst and regular spiking evoked by dendritic depolarization in layer 5 cortical pyramidal neurons. *J Neurophysiol* 81: 1341–1354, 1999.

Schwindt PC, Spain WJ, and Crill WE. Effects of intracellular calcium chelation on voltage-dependent and calcium-dependent currents in cat neocortical neurons. *Neuroscience* 47: 571–578, 1992.

Schwindt PC, Spain WJ, Foehring RC, Chubb MC, and Crill WE. Slow conductances in neurons from cat sensorimotor cortex in vitro and their role in slow excitability changes. *J Neurophysiol* 59: 450–467, 1988b.

Schwindt PC, Spain WJ, Foehring RC, Stafstrom CE, Chubb MC, and Crill WE. Multiple potassium conductances and their functions in neurons from cat sensorimotor cortex in vitro. *J Neurophysiol* 59: 424–449, 1988a.

Silva LR, Amitai Y, and Connors BW. Intrinsic oscillations of neocortex generated by layer 5 pyramidal neurons. *Science* 251: 432–435, 1991.

Singer W. Synchronization of cortical activity and its putative role in information processing and learning. *Annu Rev Physiol* 55: 349–374, 1993.

Singer W and Gray CM. Visual feature integration and the temporal correlation hypothesis. *Annu Rev Neurosci* 18: 555–586, 1995.

Spain WJ, Schwindt PC, and Crill WE. Anomalous rectification in neurons from cat sensorimotor cortex in vitro. *J Neurophysiol* 57: 1555–1576, 1987.

Spain WJ, Schwindt PC, and Crill WE. Post-inhibitory excitation and inhibition in layer V pyramidal neurones from cat sensorimotor cortex. *J Physiol* 434: 609–626, 1991a.

Spain WJ, Schwindt PC, and Crill WE. Two transient potassium currents in layer V pyramidal neurones from cat sensorimotor cortex. *J Physiol* 434: 591–607, 1991b.

Stafstrom CE, Schwindt PC, and Crill WE. Repetitive firing in layer V neurons from cat neocortex in vitro. *J Neurophysiol* 52: 264–277, 1984a.

Stafstrom CE, Schwindt PC, Flatman JA, and Crill WE. Properties of subthreshold response and action potential recorded in layer V from cat sensorimotor cortex in vitro. *J Neurophysiol* 52: 244–263, 1984b.

Steriade M. *The Intact and Sliced Brain.* Cambridge, MA: The MIT Press, 2001.

Steriade M, Amzica F, and Contreras D. Synchronization of fast (30–40 Hz) spontaneous cortical rhythms during brain activation. *J Neurosci* 16: 392–417, 1996.

Steriade M, Amzica F, and Nunez A. Cholinergic and noradrenergic modulation of the slow (approximately 0.3 Hz) oscillation in neocortical cells. *J Neurophysiol* 70: 1385–1400, 1993a.

Steriade M, Curró Dossi R, and Nunez A. Network modulation of slow intrinsic oscillation of cat thalamocortical neurons implicated in sleep delta waves: cortically induced synchronization and brainstem cholinergic suppression. *J Neurosci* 11: 3200–3217, 1991b.

Steriade M, Curró Dossi R, Paré D, and Oakson G. Fast oscillations (20–40 Hz) in thalamocortical systems and their potentiation by mesopontine cholinergic neclei in the cat. *Proc Natl Acad Sci USA* 88: 4396–4400, 1991a.

Steriade M, McCormick DA, and Sejnowski TJ. Thalamocortical oscillations in the sleeping and aroused brain. *Science* 262: 679–685, 1993b.

Steriade M, Timofeev I, Durmuller N, and Grenier F. Dynamic properties of corticothalamic neurons and local cortical interneurons generating fast rhythmic (30–40 Hz) spike bursts. *J Neurophysiol* 79: 483–490, 1998.

Stevens CF and Wang Y. Facilitation and depression at single central synapses. *Neuron* 14: 795–802, 1995.

Sutor B and Zieglgansberger W. A low-voltage activated, transient calcium current is responsible for the time-dependent depolarizing inward rectification of rat neocortical neurons *in vitro*. *Pfluegers Arch* 410: 102–111, 1987.

Taira M and Georgopoulos AP. Cortical cell types from spike trains. *Neurosci Res* 17: 39–45, 1993.

Tamas G, Buhl EH, Lorincz A, and Somogyi P. Proximally targeted GABAergic synapses and gap junctions synchronize cortical interneurons. *Nat Neurosci* 3: 366–371, 2000.

Thomson AM, Deuchars J, and West DC. Single axon excitatory postsynaptic potentials in neocortical interneurons exhibit pronounced paired pulse facilitation. *Neuroscience* 54: 347–360, 1993.

Traub RD, Jefferys JGR, and Whittington MA. *Fast Oscillations in Cortical Circuits.* Cambridge, MA: The MIT Press, 1999.

Tseng GF and Prince DA. Heterogeneity of rat corticospinal neurons. *J Comp Neurol* 335: 92–108, 1993.

Wang XJ. Fast burst firing and short-term synaptic plasticity: a model of neocortical chattering neurons. *Neuroscience* 89: 347–362, 1999.

Wang Z and McCormick DA. Control of firing mode of corticotectal and corticopontine layer V burst-generating neurons by norepinephrine, acetylcholine, and 1S,3R-ACPD. *J Neurosci* 13: 2199–2216, 1993.

Wetmore DZ and Baker SN. Post-spike distance-to-threshold trajectories of neurons in monkey motor cortex. *J Physiol* 555: 831–850, 2003.

Woody CD and Gruen E. Characterization of electrophysiological properties of intracellularly recorded neurons in the neocortex of awake cats: a comparison of the response to injected current in spike overshoot and undershoot neurons. *Brain Res* 158: 343–357, 1978.